16th World Conference on Earthquake, 16WCEE 2017

Santiago Chile, January 9th to 13th 2017

Paper N° 1188 (Abstract ID)

Registration Code: S-XXXXXXXX

NUMERICAL STUDY ON SEISMICALLY ISOLATED LIQUID-FILLED CONICAL ELEVATED TANKS

M. Moslemi[(1)], R. Kianoush[(2)]

[(1)] *Postdoctoral Fellow, Ph.D., mmoslemi@ryerson.ca*
[(2)] *Professor, Ph.D., P.Eng., kianoush@ryerson.ca*

Abstract

In this study, the applicability of seismic isolation using lead-rubber and elastomeric bearings to conical elevated tanks is investigated. The effect of seismic isolation on dynamic response of such tanks is investigated by performing finite element (FE) time-history analyses on various models. The proposed FE method is capable of simulating the accurate three-dimensional behaviour of the isolated tanks involving the nonlinear hysteretic behaviour of seismic isolators. Through this study, the effects of different parameters on the effectiveness of the seismic isolation system are investigated. The examined parameters include: lateral versus vertical isolation, locations of isolators, shaft stiffness, and tank aspect ratio. It is concluded that the application of passive control devices to conical elevated water tanks could offer a substantial benefit for the earthquake-resistant design of such structures. The obtained results further show that the magnitude and distribution of seismically induced forces, moments and displacements could be controlled through appropriate selection of device properties, isolators' locations, and tank's structural and geometrical characteristics.

Keywords: seismic isolation; conical elevated tanks; finite element; dynamic response; time-history analysis.

1. Introduction

The conventional method for earthquake-resistant design of elevated water tanks is to increase the strength of the structure so that it can tolerate the design earthquake safely. As a result of this strengthening, higher seismic forces will be applied to the structure. Contrarily, the effect of seismic input can be significantly reduced using seismic isolation technique. The seismic isolation system acts as a filter reducing the transmission of the seismically induced force to the structure.

Detailed information regarding the design methods and guidelines associated with seismic isolation of buildings may be found in a comprehensive book written by Kelly [1]. Kim and Lee [2] conducted an experimental study on isolated liquid containers. The tanks were isolated by laminated rubber bearings. The seismic isolation was found to be quite effective in reducing the dynamic response. Aiken et al. [3] tested three different types of bearings; two types of high-damping rubber bearings and one type of lead-rubber bearing. The results of the study could provide the isolation system designers with an extensive database on the mechanical characteristics and behavior of these types of isolation bearings. The seismic performance of ground-supported tanks having various isolation and energy dissipation mechanisms was further investigated by Malhotra [4-6]. Shenton III and Hampton [7] studied the seismic response of isolated elevated water tanks using a discrete three-DOF model. However, only a linear elastic isolation system was considered. Furthermore, the tank walls were assumed to be rigid and the effect of rocking of the tower on dynamic response was ignored. Shirmali and Jangid [8] investigated the seismic behavior of isolated elevated tanks under real earthquake excitations using a four-DOF model. The fluid domain was modeled as lumped masses. It was observed that the seismic response of the isolated tanks was reduced significantly. In a recent study by Waghmare et al. [9] the seismic response of isolated cylindrical water tanks with framed staging was investigated. The tanks were isolated using elastomeric bearings. The applied isolation technique was found quite effective in reducing the seismic response. The application of other types of isolation systems such as variable frequency pendulum isolators (VFPIs), and variable as well as conventional friction pendulum systems (VFPSs and FPSs) to liquid containers was also investigated extensively by Panchal and Jangid [10, 11].

Most of the available research works on seismic isolation are focused on ground supported tanks. There are only few studies on isolated elevated tanks most of which are based on simplified lumped mass models. Employing such simplified models may result in inaccuracies in calculating the actual dynamic behavior of such structures. In the current study, the seismic isolation of elevated water tanks using lead-rubber and elastomeric bearings is discussed in detail using a rigorous finite element model (FEM). The accuracy of the proposed FEM in the analysis of fluid structure interaction problems for tanks rigidly anchored to the rigid base was verified in previous studies by the authors [12-15]. The results of the present research work can provide valuable information on the actual behaviour of isolated elevated tanks under seismic motions. This study also leads to some recommendations in obtaining the optimum design of the tank and its seismic isolation system.

2. Numerical modeling

2.1 Finite element idealization of the tank-liquid system

The theory of velocity potential is used to investigate the fluid-structure interaction (FSI) problem. The linearized free surface boundary condition is considered in estimating the sloshing response. Based on the velocity potential theory, the wave equation inside the fluid domain can be defined as:

$$\nabla^2 p(x, y, z, t) = 0 \tag{1}$$

where, p is the hydrodynamic pressure, x, y, z are three-dimensional space coordinates and t is time. As explained in detail by Moslemi and Kianoush [15], the dynamic elemental equation of motion of the structure subjected to external dynamic forces can be written in matrix form as:

$$[M_e]\{\ddot{u}_e\} + [C_e]\{\dot{u}_e\} + [K_e]\{u_e\} - [R_e]\{p_e\} = \{F_e\} \tag{2}$$

where, $[M_e]$, $[C_e]$, and $[K_e]$ are elemental mass, damping, and stiffness matrices, respectively. $\{u_e\}$, $\{\dot{u}_e\}$, and $\{\ddot{u}_e\}$ are displacement, velocity, and acceleration vectors. $[R_e]$ is the coupling matrix which relates the pressure of the fluid and the forces on the fluid-structure interface. $\{p_e\}$ represents the nodal hydrodynamic pressure vector while $\{F_e\}$ denotes the elemental load vector. The hydrodynamic pressure along the fluid-structure interface is related to dynamic motions using the following boundary condition:

$$\frac{\partial p(x,y,z,t)}{\partial n} = -\rho_l a_n(x,y,z,t) \tag{3}$$

in which, ρ_l is the fluid density, and a_n is the acceleration component on the boundary along the direction outward normal n. The following boundary condition accounts for the sloshing effect on the fluid free surface assuming the small-amplitude wave condition:

$$\frac{1}{g}\frac{\partial^2 p}{\partial t^2} + \frac{\partial p}{\partial z} = 0 \tag{4}$$

where, g is the acceleration due to gravity and z represents the vertical direction. The direct integration technique using the Newmark method is employed to solve the FE discretized equations. The general purpose computer code ANSYS [16] is used to implement FE analyses. The tank structure is modeled using four-node quadrilateral shell elements and the fluid domain is modeled using eight-node isoparametric pressure-based brick fluid elements in a three dimensional space.

2.2 Modeling nonlinear behavior of elastomeric and lead-rubber bearings

Elastomeric bearings are usually made with alternating relatively thin horizontal layers of rubber bonded to horizontal steel plates. A lead-rubber bearing is manufactured by inserting a lead plug down the centre of a laminated elastomeric bearing. This introduces a significant amount of hysteretic damping to the bearing leading to further improvement in the reduction of forces and moments.

The behavior of rubber material is simulated using an appropriate hyperelastic model. The strain energy potentials are usually used to define the constitutive behavior of hyperelastic materials. In this study, the Ogden potential constitutive model [17, 18] is used for large-strain analysis of rubber. Rubber material constants are usually derived using experimental stress-strain data. In the current study, the test data reported by Treloar [19, 20] are used to characterize the rubber material constants.

Solid 185 from the ANSYS library of elements is used for the 3D FE modeling of the lead, steel, and rubber parts of the bearings. The element is capable of modeling both plasticity and hyperelasticity behaviors. The “classical bilinear kinematic hardening” plasticity algorithm is adopted to capture the nonlinear behavior of mild steel and lead materials. This plasticity algorithm uses the Von Mises yield criterion together with the kinematic hardening rule.

In order to validate the FE implementation process, the results obtained through FE analysis are compared with those measured through experiments. The considered bearing is a large circular lead-rubber shear damper with the diameter of 650 mm and the height of 197mm as shown in Fig. 1. In an experiment carried out on this bearing by Robinson [21], a high vertical load of 3.15 MN was applied first followed by the shearing force. As indicated in Fig. 1, a good agreement between Robinson experimental values and current FE results is obtained. As a result, the proposed FE method can be used to predict the response of a typical rubber bearing without the need for time consuming expensive experiments.

However, employing such a detailed FE model of bearings for dynamic analysis of a typical tank-liquid system which in turn involves a large number of finite elements is not computationally cost-effective and therefore is not practical. As a result, a practical idealization for modeling the seismic behavior of passive control bearings using a simplified two-node link element model (Link 180) is proposed here. This element has plasticity, and large strain capabilities and is capable of simulating the shearing behavior of the dissipation

devices with acceptable level of accuracy. The axial (vertical) behavior of the bearings is simulated using a two-node linear elastic spring element (Combin 14). Based on the proposed simplified modeling technique, only a vertical stiffness (Kv) is sufficient to characterize the axial behavior of the bearings. However, three main parameters are needed to define the horizontal behavior of the bearings; namely the yield strength (Qy), the elastic (Ke) and plastic (Kp) stiffnesses.

Based on the Robinson's experimental study [21], the following parameters are suggested for simplified modeling of the 650 (Diameter)×197 mm circular bearing which is used in this study for seismic isolation of the elevated tank models as discussed in the next section:

Qy = 224 kN, Ke =17 kN/mm, Kp = 2 kN/mm, and Kv = 600 kN/mm

The hysteretic behavior of the bearing using the simplified approach is also indicated in Fig. 1. As evident from the figure, a reasonable agreement is observed between the results predicted by the simplified model and experimental observations.

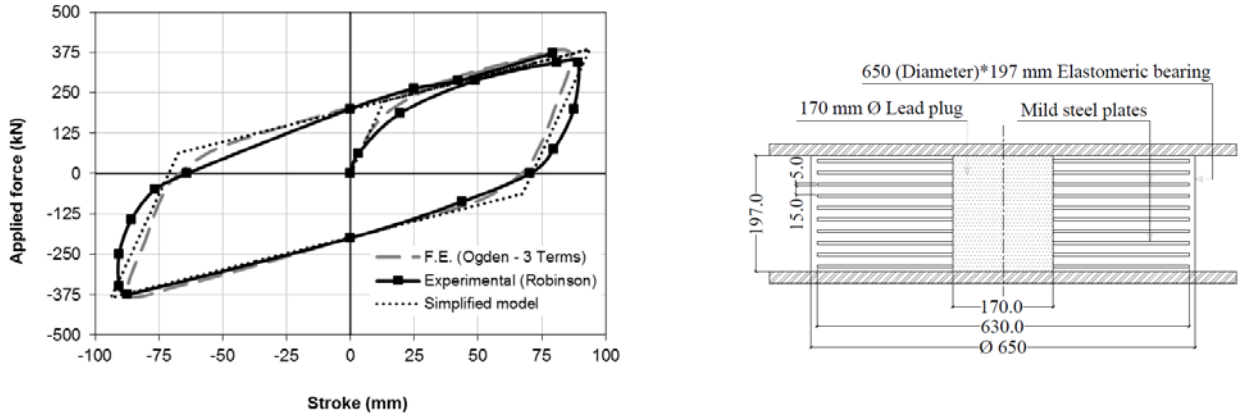

Fig. 1 – Simplified geometry and force-displacement diagram of the 650 (Diameter)×197 mm lead-rubber bearing

3. Application to liquid-filled conical elevated tanks

The particular elevated tank configuration considered for this study is that of an actual storage tank located in the U.S. with the full capacity of 7571 m^3 (2 MG) as shown in Fig. 2. Other geometric properties not given in the figure are as follows:

side shell thickness (steel)=8.8 mm; cone thickness (steel)=24.5 mm; dome floor thickness (concrete)=330 mm; pedestal thickness (concrete)=380 mm

A total of forty eight 650 (Diameter)×197 mm lead-rubber bearings are used for seismic isolation of the tank (see Fig. 2). The number and properties of the bearings are calculated based on Meggett [22] who suggests that reasonable range for the plastic shear stiffness (Kp) and the yield strength (Qy) of lead-rubber pads should be taken as:

$$Kp = (1 \text{ to } 2)\ W\ m^{-1} \quad \text{and} \quad Qy = (0.05 \text{ to } 0.10)\ W \tag{5}$$

where, W is the part of the weight carried by the bearing. In the present study, the bearings are measured with Kp = 1.1 W m^{-1} and Qy = 0.1 W.

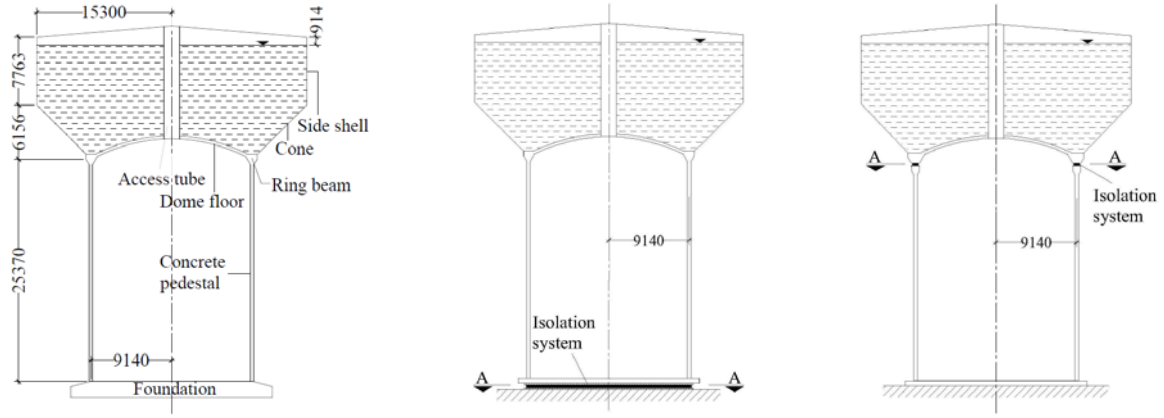

(a) (b) (c)

Fig. 2 – Simplified geometry of the tank model (all dimensions in "mm"); (a) Non-isolated, (b) Isolation type A, (c) Isolation type B

The ground motion used for the time history analysis of the tanks is the horizontal component of 1940 El-Centro ground motion scaled to the peak ground acceleration of 0.50g.

3.1 Effect of lateral and vertical isolation on dynamic response

The considered tank model is isolated at top of the shaft structure immediately below the ring beam using two different isolation techniques; vertical and lateral as shown in Fig. 2(c). Lead-rubber bearings are used for lateral isolation while elastomeric bearings are employed for vertical isolation. The dimensional properties of the considered elastomeric bearings are similar to those of lead-rubber bearings except that they do not have a lead plug at the center. The same number of isolators (n = 48) is used in both lateral and vertical isolation cases. In the case of vertical isolation no relative movement in redial direction can happen between the vessel at the top and the pedestal at the bottom. However, vertical relative displacement is free to occur. On the other hand, in lateral isolation case, the structural parts located on top and bottom of the isolators are free to move relative to each other in both radial and vertical directions. The absolute maximum time history response values corresponding to the isolated and non-isolated models are summarized in Table 1. The numbers in bold show an increase (positive) or decrease (negative) percentage over the corresponding non-isolated model.

Table 1 – Summary of peak time history response values

Response	Fixed	Laterally isolated	Vertically isolated
Base Shear (kN)	60251	19250 **(-68%)**	40830 **(-32%)**
Base Moment (kNm)	2326509	583244 **(-75%)**	1416708 **(-39%)**
Tower Drift (mm)	32.4	15.0 **(-54%)**	20.3 **(-37%)**
Displacement at tank floor level (mm)	32.4	74.3 **(+129%)**	19.4 **(-40%)**

Examining the obtained results, it can be concluded that the base shear, base moment and tower drift response values are significantly reduced due to seismic isolation in both laterally and vertically isolated models. It can further be observed that in general more reduction is achieved by the lateral isolation strategy as compared to the vertical isolation technique. However, a different trend is observed for the lateral displacement response. As shown in the table, the absolute maximum value of lateral displacement is increased by 129% in lateral isolation case while it is reduced by 40% in the case of vertical isolation. This can be the main advantage of vertical isolation over lateral isolation strategy which offers a beneficial solution to the difficulties which arise from the excessive deformations usually experienced in isolated structures. It can be concluded that when excessive deformation due to lateral isolation is not of concern, lateral isolation strategy is usually a better option

leading to a more effective solution to the problem. On the other hand, if additional structural movements cannot be accommodated by existing tank design, vertical isolation scheme is preferred.

In order to investigate the effect of seismic isolation on sloshing response, the time history sloshing height is calculated for laterally isolated model and is compared against that of non-isolated case. As a result of isolation, the free-surface displacement increases by 25% from 761mm to 955mm. This in turn results in an increase in the magnitude of convective pressure by about 33% at the water free surface. However, the maximum total hydrodynamic pressure is reduced considerably by about 80% due to lateral isolation. This could be interpreted as a stronger coupling observed between the longer period dominant isolation mode and the fundamental convective mode in the isolated tank case in comparison to the totally uncoupled (well-separated natural periods) fundamental impulsive and convective modes usually observed in typical fixed base tanks.

3.2 Effect of the location of isolators on dynamic response

In order to find the optimum location of the isolators, two different isolation schemes named as isolation type A and B are investigated. Type A bearings are located at the base of the shaft while Type B isolators are provided at top of the shaft immediately below the ring beam as shown in Figs. 2(b) and 2(c). The absolute maximum FE time history response values corresponding to the isolated and non-isolated models are given in Table 2.

Table 2 – Peak time history response values considering different locations for isolators

Response	Fixed	Isolation type B	Isolation type A
Base Shear (kN)	60251	19250 **(-68%)**	16278 **(-73%)**
Base Moment (kNm)	2326509	583244 **(-75%)**	515243 **(-78%)**
Tower Drift (mm)	32.4	15.0 **(-54%)**	21.2 **(-35%)**
Displacement at tank floor level (mm)	32.4	74.3 **(+129%)**	88.3 **(+173%)**

As obvious from the table, base shear and base moment values are reduced significantly for both isolation types. However, generally, more reduction is achieved by isolation type A as compared to type B. A different trend is observed for tower drift response. In terms of displacement at tank floor level, isolation type B is considered to be advantageous over type A. The obtained force-displacement hysteretic loops corresponding to isolation types A and B are given in Fig. 3. From the figure, the maximum absolute bearing displacements for isolation types A and B are found to be 68 mm and 60 mm, respectively. The area enclosed in a hysteretic loop implies the energy dissipated in a cycle.

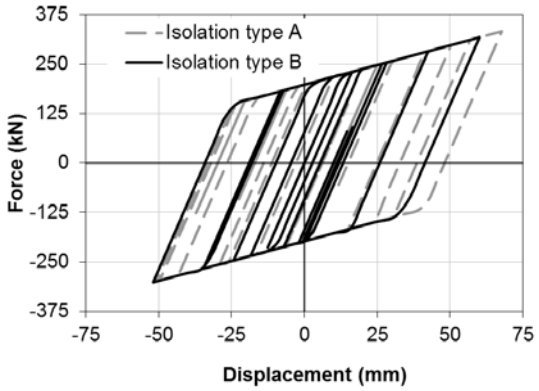

Fig. 3 – Hysteretic diagrams for isolation types A and B

Therefore, it can be concluded from the figure that the total amount of energy absorbed during the earthquake increases when isolators are located at the base of the shaft as compared to the case where they are

installed at top of the shaft. This could be considered as an advantage for isolation type A over type B. The reason can be attributed to the increase in vertical loads applied to the isolators due to the self-weight of the shaft, weight of platforms inside the shaft and their live load, and the weights of all other accessories attached to the shaft structure. This phenomenon has also been observed experimentally in research works by Robinson [21] and King [23].

3.3 Effect of stiffness of the shaft structure on dynamic response

To investigate this effect, two tank models having different shaft stiffness characteristics namely; "stiff" and "flexible" are considered and their time history response is calculated using the proposed FE methodology. Models are assumed to be laterally isolated at top of the shaft and the same isolation properties are considered for both models. The properties of the considered isolation system are as explained before. The flexible model is created by reducing the shaft stiffness as low as one third of that of the original model (stiff model). All other properties of the two models are assumed to be the same. Table 3 lists the peak time history response values obtained for the isolated stiff and flexible models against those of corresponding non-isolated models. From the table, it can be observed that the reduction in dynamic response due to seismic isolation is comparatively more pronounced in stiff model.

Table 3 – Peak time history response values for stiff and flexible models

	Stiff		Flexible	
Response	Fixed	Isolated	Fixed	Isolated
Base Shear (kN)	60251	19250 (**-68%**)	35182	16156 (**-54%**)
Base Moment (kNm)	2326509	583244 (**-75%**)	1266423	518286 (**-59%**)
Tower Drift (mm)	32.4	15.0 (**-54%**)	59.5	45.3 (**-24%**)

The peak base shear and base moment response values calculated for the isolated tanks are compared against those of non-isolated tanks for two different values of shaft stiffness, as indicated in Fig. 4. As obvious from the figure, the response of isolated tanks is obviously less sensitive to the flexibility of the shaft structure as compared to the corresponding non-isolated tanks. In other words, the dynamic response of isolated tanks is not significantly influenced by the stiffness properties of the supporting shaft structure.

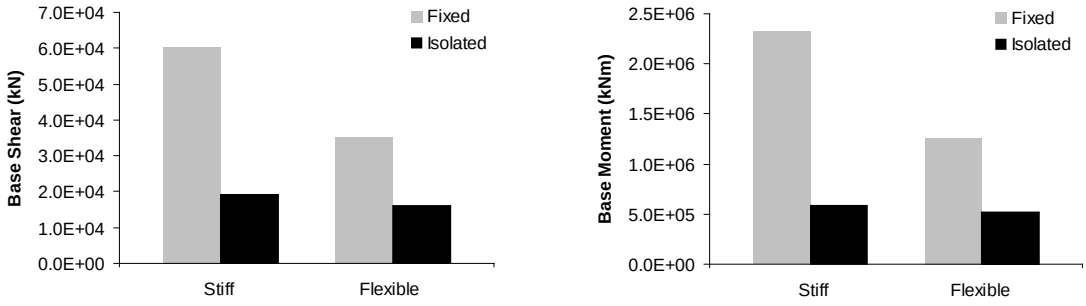

(a) (b)

Fig. 4 – Comparison of results between stiff and flexible tank models

3.4 Effect of tank aspect ratio

In order to investigate the sensitivity of seismic isolation to the tank's geometry, the transient response of two tank models having different aspect ratios namely; "broad" and "slender" is determined in both isolated and non-isolated conditions. The effectiveness of seismic isolation is then examined by comparing the obtained results. The considered broad and slender models have the aspect ratios of 0.7 and 2.1, respectively. Tank aspect ratio (A.R.) is defined as the ratio of equivalent water height (based on the concept of equivalent cylinder model as stated in ACI 371R-08 [24]) to the radius of the cylindrical part of the vessel. The simplified geometries of the

broad and slender models are shown in Figs. 2 and 5, respectively. The tanks are assumed to be laterally isolated at top of the shaft, and the same isolation properties are considered for both models as explained before.

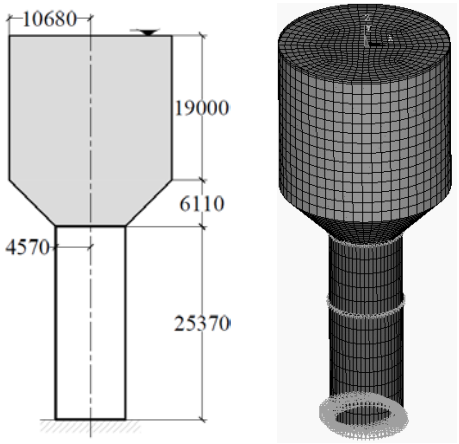

Fig. 5 – Simplified geometry and FE idealization of the slender tank model

The volume of contained water is the same in both cases. Furthermore, the stiffness and mass distributions along the height of the shaft, and conical and cylindrical side shells are similar for both models. The mass distributions are made equivalent by adjusting the mass density of each section (shaft, cone, and cylinder parts) of the tank appropriately. As a result of this adjustment, the total weight of the structure will be the same for both models. The stiffness distributions are also made equivalent by altering the thickness of each shell section (shaft, cone, and cylinder parts) properly such that the concerning stiffness becomes equal to that of the other model. These adjustments result in equal values of shaft period, isolation time period, and isolation yield strength for both models. As a result, the obtained time history results are considered to be readily comparable. Table 4 lists the peak time history response values of the isolated broad and slender models against corresponding non-isolated ones.

Table 4 – Peak time history response values for broad and slender tank models

Model		Bearing Disp. (mm)	Sloshing Disp. (mm)	Base Shear (kN)	Base Moment (kNm)	Tower Drift (mm)
Broad	Fixed	NA	761	60251	2326509	32.4
	Isolated	60	955 **(+25%)**	19250 **(-68%)**	583244 **(-75%)**	15.0 **(-54%)**
Slender	Fixed	NA	844	88810	3211956	36.9
	Isolated	83	1148 **(+36%)**	20785 **(-77%)**	690779 **(-79%)**	8.2 **(-78 %)**

As presented in the table, the base shear and base moment values of slender model are greater than those of broad model in both fixed and isolated conditions. This reveals the significant effect of tank geometry on the dynamic response of the elevated tanks in both fixed and isolated conditions. Moreover, it can be concluded that comparatively greater reductions in dynamic response can be achieved due to seismic isolation in slender tank as compared to broad tank.

As shown in Fig. 6, as a result of seismic isolation, the free-surface displacement of slender model increases by about 36% from 844mm to1148mm, while this value is about 25% in broad tank model. This difference may be due to a stronger coupling between the fundamental sloshing mode and the isolation mode in tank with higher aspect ratio (slender model) as compared to that with lower aspect ratio (broad model).

Fig. 7 shows the force-displacement hysteretic loops during the earthquake corresponding to broad and slender models. As obvious from the figure, the total amount of absorbed energy increases for the tank with higher aspect ratio. This could be considered as another advantage for slender tanks over broad tanks in seismic isolation applications.

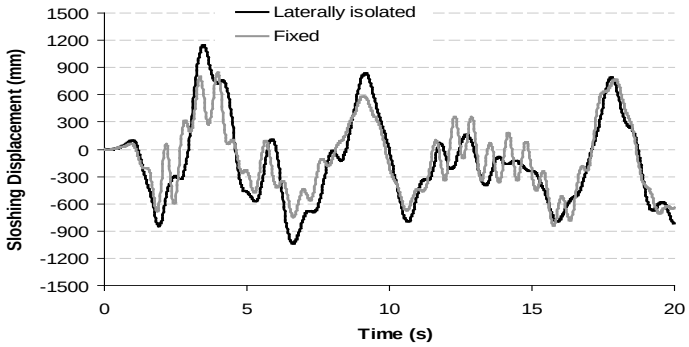

Fig. 6 – Time history of sloshing height at water free surface (slender tank)

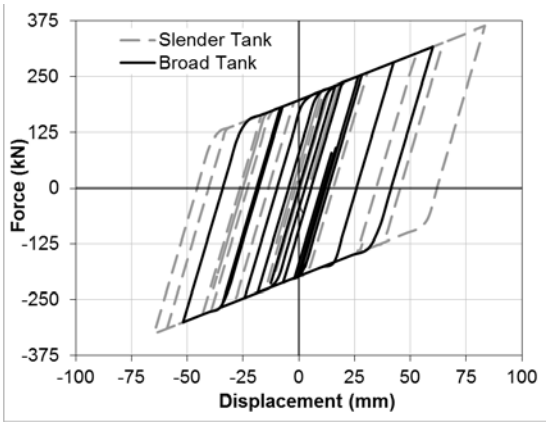

Fig. 7 – Hysteretic diagrams for broad and slender models

4. Conclusions

The complex dynamic behavior of isolated liquid-filled elevated tanks is investigated using a rigorous FE method capable of accounting for the fluid-structure interaction effect as well as the nonlinear response of isolation system. It is well observed that the application of passive control devices to conical elevated tanks could offer a substantial benefit for the earthquake-resistant design of such structures. Despite its efficiency in reducing the seismic response, the obtained results suggest an increase in the sloshing height and as a result the convective component of pressure due to isolation effect. This may be considered as a drawback for the isolated elevated tank systems as compared to the typical fixed-base tanks. However, this amplification effect is negligible for the properly designed isolated tanks with well separated base isolation and liquid sloshing frequencies. Moreover, this increase in sloshing response is offset by the reduction in impulsive response yielding to a considerable net decrease in total response. Comparing the response of laterally and vertically isolated tanks, one can suggest that when excessive deformation due to lateral isolation is not of concern, this isolation strategy is usually a better option leading to a more effective solution. The effect of the location of isolators whether provided at the base or top of the shaft is found to be inconclusive. Shaft stiffness is to be considered as a key factor affecting the efficiency of the isolation system; that is, the higher the stiffness of the shaft the higher the efficiency of the isolation system. The calculated results further suggest that slender tanks may be more favorable in terms of being more effective isolation systems as compared to broad tanks of the same capacity.

It is important to note that the conclusions drawn in this study should be considered valid only within the defined scope of the paper. As a continuation to the present work it is recommended to conduct a comprehensive parametric study covering a wider range of deciding parameters of an isolated elevated tank system such as tank

capacity, tank geometry, shaft stiffness, as well as isolator stiffness and yield strength based on the needs imposed by today's practice.

5. References

[1] Kelly JM (1997): *Earthquake-Resistant Design with Rubber*. Springer-Verlag, London.

[2] Kim NS, Lee DG (1995): Pseudo-dynamic test for evaluation of seismic performance of base-isolated liquid storage tanks. *Engineering Structures*, **17**(3), 198-208.

[3] Aiken ID, Kelly JM, Clark PW, Tamura K, Kikuchi M, Itoh T (1992): Experimental studies of the mechanical characteristics of three types of seismic isolation bearings. *Proc. 10th WCEE*, Madrid, Spain.

[4] Malhotra PK (1997): Method for seismic base isolation of liquid storage tanks. *J. Struct. Engrg*., ASCE, **123**(1), 113-116.

[5] Malhotra PK (1997): New method for seismic isolation of liquid storage tanks. *Journal of Earthquake Engineering and Structural Dynamics*, **26**, 839-847.

[6] Malhotra PK (1998): Seismic strengthening of liquid storage tanks with energy-dissipating anchors. *J. Struct. Engrg.*, ASCE, **124**(4), 405-414.

[7] Shenton III HW, Hampton FP (1999): Seismic response of isolated elevated water tanks. *ASCE Journal of Structural Engineering*, **125**(9), 965-976.

[8] Shirmali MK, Jangid RS (2003): The seismic response of elevated liquid storage tanks isolated by lead-rubber bearings. *Bulletin of the New Zealand Society of Earthquake* Engineering, 141-164.

[9] Waghmare PB, Pajgade PS, Kanhe NM (2013): Seismic response of isolated liquid storage tanks with elastomeric bearings. *International Journal of Application or Innovation in Engineering & Management*, **2**(2).

[10] Panchal VR, Jangid RS (2008): Variable friction pendulum system for seismic isolation of liquid storage tanks. *Nuclear Engineering and Design*, **238**(6), 1304-1315.

[11] Panchal VR, Jangid RS (2011): Seismic response of liquid storage steel tanks with variable frequency pendulum isolator. *KSCE Journal of Civil Engineering*, **15**(6), 1041-1055.

[12] Ghaemmaghami AR, Moslemi M, Kianoush MR (2010): Dynamic behaviour of concrete liquid tanks under horizontal and vertical ground motions using finite element method. *9th US National and 10th Canadian Conf. on Earthquake Eng.*, Toronto, Canada.

[13] Moslemi M, Kianoush MR, Pogorzelski W (2011): Seismic response of liquid-filled elevated tanks. *Journal of Engineering Structures*, **33**(6), 2074-2084.

[14] Moslemi M (2011): Seismic response of ground cylindrical and elevated conical reinforced concrete tanks. PhD Thesis, Civil Engineering, Ryerson University, Toronto, Ontario, Canada.

[15] Moslemi M, Kianoush MR (2012): Parametric study on dynamic behavior of cylindrical ground-supported tanks. *Journal of Engineering Structures*, **42**, 214-230.

[16] ANSYS Ver. 16.2 (2015): SAS IP Inc. ANSYS Multiphysics, Houston, PA.

[17] Ogden RW (1984): *Nonlinear Elastic Deformations*. Dover Publications, Inc.

[18] Ogden RW (1986): Recent advances in the phenomenological theory of rubber elasticity. *J. Rubber Chem. Technol.*, **59**, 361-383.

[19] Treloar LRG (1944): Stress-strain data for vulcanized rubber under various types of deformations. *Trans. Faraday Soc*., **40**, 59-70.

[20] Treloar LRG (1975): *The physics of rubber elasticity*. Oxford, Clarendon Press.

[21] Robinson WH (1982): Lead-rubber hysteretic bearings suitable for protecting structures during earthquakes. *Earthquake Engrg. and Struct. Dyn*., **10**, 593-604.

[22] Meggett LM (1978): Analysis and design of a base-isolated reinforced concrete frame building. *Bulletin of the New Zealand Society of Earthquake Engineering*, **11**, 245-254.

[23] King PG (1980): Mechanical energy dissipation for seismic structures. *Report 228*, Department of Civil Engineering, University of Auckland, Auckland.

[24] ACI Committee 371 (2008): Guide for the analysis, design and construction of elevated concrete and composite steel-concrete water storage tanks (ACI 371R-08). American Concrete Institute, Farmington Hills, MI, USA.